Available online at www.CivileJournal.org

Civil Engineering Journal

(E-ISSN: 2476-3055; ISSN: 2676-6957)

Vol. 9, No. 11, November, 2023

A Comparative Study on the Optimal Modeling of Laminated Glass

Moheldeen A. Hejazi [1*], Ali Sari [2]

[1] *Ph.D. Candidate in Structural Engineering at the Civil Engineering Department, Istanbul Technical University, Turkey.*

[2] *Associate Professor at the Civil Engineering Department, Istanbul Technical University, Turkey.*

Received 08 May 2023; Revised 12 October 2023; Accepted 19 October 2023; Published 01 November 2023

Abstract

This study addresses the challenging task of modeling laminated glass responses to extreme loading scenarios for the design and analysis of protective structures. The primary objective is to seek an optimal modeling approach that balances accuracy and computational efficiency. To achieve this, the failure modeling of laminated glass layups comprising thin and thick panels with three and eleven layers is investigated under blast loading conditions. Various simulation techniques are employed, including the finite element method (FEM) with element erosion/deletion, smoothed particle hydrodynamics (SPH), and a hybrid approach involving the conversion of elements into particles. The feasibility and limitations of each technique are examined, considering both accuracy and computational cost. Experimental results from arena and shock tube testing scenarios assess the deployed modeling techniques and the presented comparisons. Emphasis is placed on mesh sensitivity and the significance of adaptive meshing in capturing fracture patterns. The present paper suggests that utilizing hybrid techniques results in optimal modeling outcomes. Furthermore, the stability of the modeling results under diverse blast conditions is confirmed. This article contributes to the field by offering insights into modeling laminated glass responses to extreme loading, emphasizing the use of hybrid techniques to strike a balance between accuracy and computational efficiency. This research enhances the understanding of protective structure design and analysis, highlighting the critical importance of computational methods in this context.

Keywords: Laminated Glass; Blast Loading; Failure Modeling; Mesh-Based Method; Mesh-Free Method; Computational Cost.

1. Introduction

Due to its safety-enhancing characteristics, laminated glass is a versatile material with applications in diverse sectors, including architecture, automotive, defense, and aerospace. It comprises brittle exterior layers and polymeric interlayers, forming a protective composite against extreme exposures [1]. Despite numerous studies, predicting laminated glass behavior under various loads remains complex due to its complex structure and behavior [2]. Recent research has investigated critical aspects including glass compositions [3]; properties and behavior [4–6]; interlayer materials and lamination [7–9]; characterization [10–12]; bonding and delamination [13, 14]; and modeling techniques [2].

Firstly, glass forms the main component in laminated glazing units [15–19]. Various models were developed to tackle the nature of annealed [20, 21] and tempered glass [22, 23] under different conditions. Characterized by its complex and highly brittle response, the vital mechanical properties of glass were investigated [2], including the tensile and flexural strengths [24], fracture toughness [25], and the probabilistic nature of glass failure [26]. On the other hand, interlayer materials play a pivotal role in laminated glazing by enhancing strength, durability, and impact resistance [27]. Another frequent component of laminated glazing units (particularly in thick multi-layered units) is the

* Corresponding author: hejazi19@itu.edu.tr

http://dx.doi.org/10.28991/CEJ-2023-09-11-018

polycarbonate material [28], which offers superior impact resistance and toughness despite being more susceptible to scratching (compared to glass). Furthermore, it increases the glazing unit's ability to absorb and disperse energy upon impact, preventing shattering [29].

Studies tackled the laminated glass behavior under varying conditions [7, 30]; high strain-rate effects [31]; constitutive models [32, 33]; fracture [34–36]; fatigue [6]; and aging [37], yielding improved understanding. Modeling the laminated glass response to blast loading is vital to understanding its response under such extreme exposures [38, 39]. The implemented numerical techniques typically fall into three broad categories [40]: continuum-based, discontinuum-based, and hybrid. The continuum-based methods include the finite elements method (FEM), the extended finite element method (XFEM), and the finite element with element deletion (FEM-ED), among others. Meanwhile, the discontinuum-based methods include the discrete element method (DEM) and smooth particle hydrodynamics (SPH). Finally, the hybrid techniques include the finite-discrete element method (FDEM) and the finite element with smooth particle hydrodynamics (FE-SPH). A brief comparison of the various modeling techniques for laminated glass is summarized in Table 1.

Table 1. Comparison of modeling techniques for laminated glass and laminated composites

Modeling Method	Main Applications	Advantages	Disadvantages
FEM [41]	Structural response, stress analysis, dynamic analysis	Widely adopted, well-established, accurate representation of complex geometries, versatile for various material behaviors	Mesh dependence, difficulties in capturing cracks and fractures, requires remeshing for crack propagation
XFEM [42]	Crack propagation analysis, fracture mechanics, progressive damage analysis	Efficient for crack propagation simulations, eliminates the need for remeshing, accurate representation of complex fractures	Complex implementation, computational overhead, requires enrichment functions for crack modeling
CDM [43]	Progressive failure analysis, impact analysis, fracture behavior modeling	Captures damage evolution, suitable for progressive failure analysis, accounts for material softening and fracture behavior	Requires constitutive models, calibration of damage parameters, may not accurately capture sudden failure or localized fractures
ED [44]	Crack initiation and propagation analysis, fracture mechanics, localized damage analysis	Captures localized fractures, suitable for crack propagation analysis, computationally efficient in certain cases	Simplified representation of crack behavior, limited applicability to specific fracture patterns or failure modes
Adaptive FE [45]	Stress concentration analysis, critical area analysis, optimization and design refinement	Efficiently captures localized features and critical areas, reduces computational cost, improves accuracy in critical regions	Additional computational cost for mesh adaptation, implementation complexity, requires careful selection of refinement and coarsening criteria
DEM [46]	Granular materials, fracture and fragmentation analysis, impact simulations	Captures granular behavior, suitable for simulating glass fracture and fragmentation	High computational cost, difficult to model complex geometries and large-scale structures, requires calibration of particle properties
FDEM [47]	Multi-scale analysis, laminated glass fracture, interfacial behavior	Allows for modeling of the continuum behavior using FEM and the discontinuous behavior using DEM, captures scale-dependent fracture phenomena	Increased computational complexity, requires calibration of interface properties, challenging to simulate dynamic loading conditions
FE-CA [48]	Fracture mechanics, crack propagation, localized damage analysis	Captures localized fracture patterns, efficient in modeling crack propagation	Complex implementation, requires calibration of parameters, limited applicability to specific fracture patterns, may not accurately capture crack branching
FE-SPH [49-51]	Fluid-structure interactions, impact simulations, blast loading analysis	Captures fluid-structure interactions, suitable for modeling glass under impact or blast loading	Computational cost, requires careful calibration of SPH parameters

This article investigates the accuracy, efficiency, and computational demand of a subset of the listed modeling techniques, namely the Finite Element Method (FEM); FEM with Element Deletion (FEM-ED); smooth particle hydrodynamics (SPH); and the hybrid Finite Element-smooth particle hydrodynamics (FEM-SPH) method. Hence, the modeling techniques considered in this study are intended as a representative subset of the modeling techniques in Table 1. These methods exhibit distinct strengths and capabilities that are highly pertinent to the specific objectives of this investigation. For example, the FEM-ED approach is recognized for accurately capturing localized fractures. In contrast, the FEM-SPH and SPH methods demonstrate exceptional performance in simulating high-velocity impact, damage, and fragmentation. The Finite Element Method (FEM), a widely adopted and well-established technique, serves as a benchmark for comparison. Moreover, selecting these methods takes into account factors such as the availability of relevant literature, computational resources, and expertise, ensuring their feasibility for implementation within the scope of this study.

This article is structured in the "Materials and Methodology" section, first highlighting material properties through monolithic glass testing and a literature review. After that, the implemented modeling techniques (FEM, SPH, FEM-ED, and FEM-SPH) are briefly introduced. The "Experimental Data" section presents the experimental data on laminated glass collected in the scope of this study through testing and from the literature. Then, the various modeling techniques are compared to the results presented in the "Results and Discussion" section. Finally, the main findings are summarized in the "Conclusions" section. The flowchart of this investigation is presented in Figure 1.

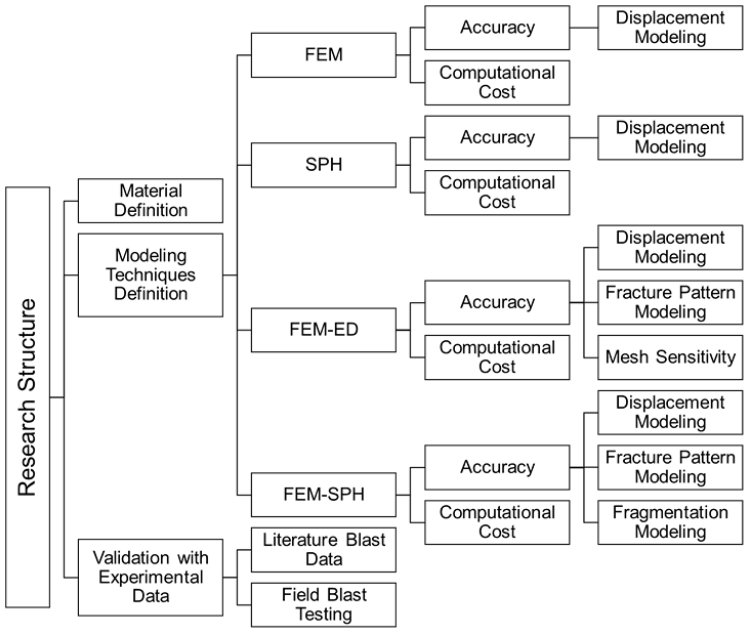

Figure 1. The flow chart of the investigation procedure

2. Materials and Methodology

This section provides an overview of the material properties modeling techniques implemented in modeling laminated glass (LG) units against blast loading (Field blast testing and shock tubes). Initial emphasis is placed on the material properties collected through monolithic glass testing and from the literature. Subsequently, the section details adopted modeling methods: Finite Element Method (FEM), Finite Element with Element Deletion (FEM-ED), smooth particle hydrodynamics (SPH), and hybrid Finite Element with smooth particle hydrodynamics (FEM-SPH).

2.1. Material Properties

Understanding the properties of the constituent materials in a laminated glass unit is crucial for accurately predicting the laminated glass's response during blast loading [52]. The laminated glass units investigated in this study were composed of soda-lime-silica annealed glass, thermoplastic polyurethane (TPU), and polyvinyl butyral (PVB) interlayers, as well as polycarbonate (PC) material. The following subsections provide a detailed analysis of the properties and behavior of these materials under blast exposure.

2.1.1. Annealed Glass

Various glass types play roles in construction, including annealed, heat-strengthened, and toughened glass [53]. In this study, annealed glass was modeled by employing an elastic-brittle cracking model. The material properties were collected through a testing program by glass manufacturer SISECAM. Chemical compositions were determined using X-ray fluorescence (XRF), analyzing characteristic fluorescent X-rays emitted when bombarded with high-energy X-rays. Composition results for soda-lime annealed glass are provided in Table 2.

Table 2. The chemical compositions of the tested soda-lime annealed glass

Component	Min	Max	Mean	SD
SiO_2	71.24	72.29	71.84	0.33
Al_2O_3	0.810	1.190	1.008	0.110
Fe_2O_3	0.063	0.081	0.071	0.003
TiO_2	0.036	0.059	0.045	0.005
CaO	8.270	8.860	8.529	0.176
MgO	4.240	4.480	4.393	0.067
Na_2O	13.570	13.920	13.739	0.072
K_2O	0.040	0.350	0.174	0.121
SO_3	0.180	0.230	0.203	0.013
$Na_2O + K_2O$	13.750	14.130	13.910	0.101
CaO / MgO	1.846	2.024	1.941	0.054

Moreover, based on the testing program for 44 annealed glass specimens in SISECAM laboratories, essential mechanical properties obtained for simulation are listed in Table 3.

Table 3. The material properties implemented in the modeling of the annealed glass layers

Parameter	Value
Density	2530 Kg/m^3 (158 lb/ft^3)
Elastic modulus	72000 MPa (10443 ksi) Quasi-static
	94500 MPa (13706 ksi) @ 1700 strain rate
Stress failure limit	110 Mpa (16 ksi)
Poisson ratio	0.22
Modulus of Toughness	0.076
Energy release rate	0.0075 millijoule/mm^2
Ultimate stress	100 MPa (14.50 Ksi)
Crack opening displacement	0.05 mm (0.002 in)

Various models were collected and tested for the annealed glass from the literature, including the straightforward brittle elastic model with a brittle cracking limit associated with the 70-100 MPa strength limit, up to the advanced damage initiation and propagation models by Johnson-Holmquist for ceramics, the model developed by Bedon et al. (2022) [54], the model developed by Hidallana-Gamage et al. [39] and others [55, 56]. The simple brittle cracking model offered satisfactory results at 47% less computational cost compared to the implementation of damage propagation models. The error recorded in the displacement was 9.4%, deemed adequate in simulating the experiments in this study

2.1.2. Polycarbonate

Polycarbonate, an amorphous polymer composed of carbonate functional groups, is synthesized via condensation polymerization of bisphenol A (BPA) and phosgene, resulting in a high molecular weight chain-like structure. Its viscoelastic and energy-damping nature allows energy absorption during impact, and its linear chain structure contributes to enhanced mechanical performance, granting notable tensile and flexural strength.

This study modeled polycarbonate as an elastic-plastic material with properties listed in Table 4. Viscoelastic effects are disregarded for computational efficiency due to high-strain rate conditions.

Table 4. A summary of the material properties of PC, PVB, and TPU

Parameter	PC	PVB	TPU	Unit
Density	1200 (74.9)	1180 (73.7)	1077 (67.2)	Kg/m3 (lb/ft^3)
Elastic modulus	2380 (345)	2400 (348)	3500 (508)	MPa (ksi)
Elastic modulus at 300 s-1	2800 (406)	2700 (392)	3800 (551)	MPa (ksi)
Poisson's ratio	0.40	0.35	0.45	-
Ductile, Ultimate hydrostatic cutoff stress	60 (8702)	60 (8702)	80 (11603)	MPa (psi)

The mechanical behavior of polycarbonate is considered at a strain rate of 300 1/s. Reference is made to Cao et al.'s (2012) study to capture material behavior accurately [55]. The experimental force-displacement curve from Cao et al.'s work is adjusted for simulation stability by fitting it to a second-degree polynomial while preserving the fracture energy release rate. The adapted force-displacement curve, alongside the original experimental curve, is displayed in Figure 2.

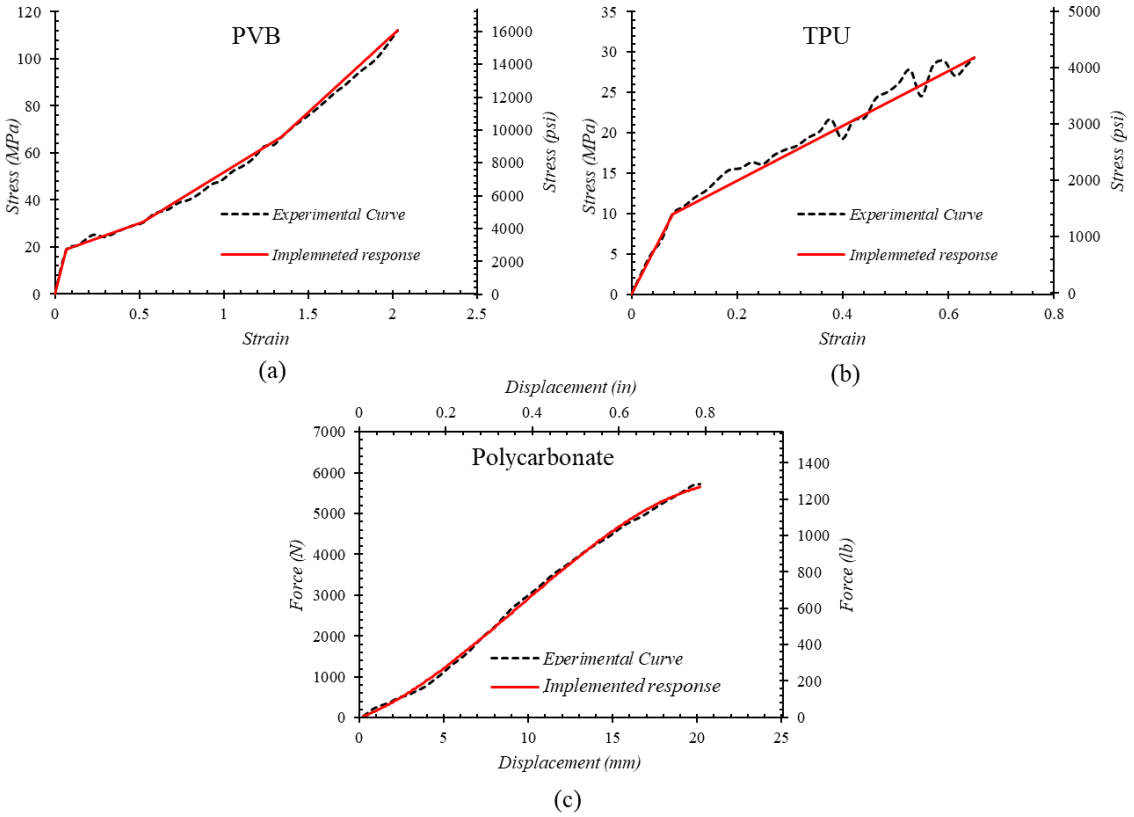

Figure 2. The response curve implemented in the analyses of (a) PVB, (b) TPU, and (c) Polycarbonate

2.1.3. Interlayer Materials

Interlayer materials significantly influence laminated glass's mechanical behavior, particularly in maintaining integrity and affecting stress distribution and energy absorption. Commonly used are polyvinyl butyral (PVB) and thermoplastic polyurethane (TPU) interlayers [7]. Their properties strongly impact laminated glass under varied loads. Thickness and interlayer material used also affect energy absorption and failure mode. This study incorporates Saflex PVB [57] and Krystalflex TPU [58] interlayers in the tested laminated glass configuration (Table 5). PVB and TPU are modeled as Plastic materials with initial elasticity up to the yielding limit. The viscoelasticity of the interlayers under High strain rates, short blast durations, and below-glass transition temperature was deemed negligible. The stress-strain curves (Figure 2) depict the mechanical behaviors of investigated interlayer materials. These properties correspond to materials tested at a high strain rate (400/s – 6500/s) and a temperature of (20-25) Celsius

Table 5. The configuration of the laminated glass unit used in the blast testing

Layer	Property	Thickness		Weight	
No.	Name	in	mm	lb.	kg
1	Polycarbonate	0.115	2.9	5.96	2.70
2	TPU KrystalFlex	0.030	0.8	1.48	0.67
3	Polycarbonate	0.115	2.9	5.96	2.70
4	TPU KrystalFlex	0.030	0.8	1.48	0.67
5	Annealed Glass	0.469	11.9	54.7	24.81
6	TPU KrystalFlex	0.030	0.8	1.48	0.67
7	Annealed Glass	0.469	11.9	54.7	24.81
8	TPU KrystalFlex	0.030	0.8	1.48	0.67
9	Annealed Glass	0.355	9.0	54.7	24.81
10	TPU KrystalFlex	0.030	0.8	1.48	0.67
11	Annealed Glass	0.355	9.0	54.7	24.81
	Total	**2.028**	**51.5**	**238.13**	**108.01**

2.2. Modeling Techniques

The process of modeling the response of laminated glass units is critical in the industry for analyzing, designing, and predicting the end response of the manufactured laminated glass under a wide range of extreme loading scenarios [2]. This study implements four modeling techniques, including FEM, FEM-ED, SPH, and FEM-SPH methods. All modeling techniques were investigated using the Abaqus-Explicit solver. The main parameters needed are summarized in Table 6. The material properties and definitions are given in the "Material Properties" section, Tables 3 and 4. The following context briefly discusses the procedure followed in each modeling technique.

Table 6. A summary of the main modeling parameters

Method	Parameter	Value
General	Constitutive models	"Material Properties" section
	Boundary conditions	Clamped/Fixed, four sides
	Static contact coefficient	0.3
	Kinematic contact coefficient	0.3
	Contact damping	0.7
	Simulation time step	Calculated minimum stable time increment
FEM	Element type	3D triangular linear elements, reduced integration, hourglass control
	Mesh size	0.1 mm ~ 1 mm Fine mesh, 10 mm ~ 50 mm coarse mesh
FEM-ED	Element deletion criteria	Maximum stress
SPH	Kernel function	Cubic spline kernel function
	Particle distribution	0.1 mm ~ 1 mm for fine modeling, 10 mm ~ 50 mm for rough predictions
FEM-SPH	Coupling method	Penalty method
	Contact algorithm	Penalty method
	Crack initiation and propagation	Allowed, Stress-based conversion threshold.

2.2.1. FEM

In this study, finite element modeling serves as a benchmark for comparison. The laminated glass assemblies were modeled using structured 3D eight-node linear elements (type C3D8R) with reduced integration and hourglass control. The adapted mesh size varied between 0.5 and 1 mm for the various assemblies. The contacting nodes between the glass and interlayers are merged. Consequently, glass debonding from the interlayer is not modeled in the simulation. This practice aligns with the findings of others [59], wherein empirical examinations involving field blast tests on laminated glass have consistently demonstrated the rare incidence of delamination between fractured glass and the interlayer. This simplification helps to improve computational efficiency, as it reduces the number of degrees of freedom in the model.

To further improve computational efficiency, an adequate thickness of the interlayers was implemented using the concept of equivalent material stiffness. This involved combining a small portion of the adjacent glass layers with the interlayers. Meanwhile, the elastic modulus of the PVB was scaled to 2400 and 2700 MPa at quasi-static and 300 1/s strain rates, respectively. Meanwhile, the elastic modulus for TPU was scaled to 3500 and 3800 for quasi-static and 300 1/s strain rates, respectively. This implementation results in a more uniform element size across the model, enhanced numerical stability, and lower computational cost.

2.2.2. Hybrid FEM-ED

The element deletion method offers crack simulation and is a widely utilized approach where an element is promptly removed when it satisfies a failure criterion. This approach has found application in simulating glass fracture and various other problems [60]. In this method, the stiffness matrix of an element is set to zero within a single time increment of meeting the failure criterion at one or more of its integration points. It does not account for damage softening or consider the crack's directionality. The Rankine principal stress criterion is employed as the fracture criterion for macroscopic linear elastic-brittle materials.

To mitigate dynamic effects during the elastic phase, an artificially high density is used to increase inertia. Moreover, the contact cohesion between the various layers was included using normal and shear penalty coefficients at the interfaces (Table 6). This adjustment also results in a higher stable time increment. In this modeling technique, the fracture strength is expected to be reached when the strain reaches 0.1% in uniaxial tension. Once the failure stress is attained, the element loses its load-bearing capacity entirely. At that moment, all strain energy within the element dissipates instantaneously as the material stiffness becomes zero. Consequently, no stress oscillations occur, and there is no viscous dissipation of energy through stress wave damping.

2.2.3. SPH

Load modeling of laminated glass. It uniquely discretizes continuum equations without relying on spatial meshes, making it well-suited for complex problems involving substantial deformations and free surfaces, such as structural issues and fragmentation. While effective, SPH may exhibit lower accuracy compared to Lagrangian finite element analyses for mild deformations and Eulerian-Lagrangian analyses for severe deformations. Challenges involve tensile instability and boundary condition definition. Tensile instability, causing unphysical particle clustering, is counteracted by introducing artificial stress through short-range repulsion. Poor kernel estimates near domain edges impacting boundary conditions are mitigated by enforcing conditions and smoothing near-edge estimations. Addressing these challenges enables SPH's reliable and accurate simulations for blast-loaded laminated glass.

In this study, SPH with a cubic kernel formulation was implemented to model the laminated glazing units. For this purpose, a 3D mesh was used to generate uniformly distributed particles through the conversion of elements to particles at time zero of the simulation.

2.2.4. Hybrid FEM-SPH

The hybrid use of the finite element method (FEM) with smoothed particle hydrodynamics (SPH) through element conversion offers a valuable approach for modeling laminated glass subjected to blast loads. This method involves converting a portion of the FEM mesh into SPH particles, allowing for an accurate representation of fragmentation and significant deformations. This conversion is performed element-wise once an element reaches a conversion threshold (e.g., Stress, strain, displacement, energy release rate). However, several challenges need to be addressed when utilizing this hybrid approach. Challenges in the hybrid FEM-SPH approach through element conversion include proper conversion techniques and enforcing interaction between the FEM and SPH regions. Remedies for these challenges involve employing appropriate penalties and damping, ensuring compatible interpolation schemes between FEM and SPH elements, and accurately mapping the physical properties from the FEM to the SPH region. Additionally, addressing potential issues related to capturing crack initiation and propagation are essential aspects to consider in this hybrid approach. By addressing these challenges and implementing their respective remedies, the hybrid FEM-SPH approach through element conversion can provide reliable and precise simulations of laminated glass under blast loads.

3. Experimental Data

3.1. Experiments from the Literature

In this study, several experimental results by others [7, 14, 61–63] were collected and examined against different modeling techniques to compare these techniques in terms of accuracy and computational efficiency. The experiments include blast testing results on three layers of annealed laminated glass panels with PVB interlayers. The panel dimensions and blast load characteristics are given in Table 7. All experiments featured a panel configuration of 3-1.52–3 (3 mm annealed glass- 1.52 mm PVB – 3 mm annealed glass) except for Larcher et al. [62] study, where the LG unit has the configuration 6- 2.28-6. In this context, only the positive phase of each experiment was considered. The negligible influence of the negative phase in all considered experiments can be attributed to the positive phase pressures surpassing the negative phase pressures by a ratio greater than 5. .

Table 7. Experimental data examined from the literature

ID	Source	Dimensions (m)	Scenario	Weight	Standoff Distance (m)	Peak Pressure (kPa)	Duration (ms)
EXP.1	Larcher-1	0.89 × 1.09	Shock tube	-	-	150	36
EXP.2	Larcher-2	0.89 × 1.09	Shock tube	-	-	105	29
EXP.3	Hooper-1	1.5 × 1.2	Blast Test	15 kg C4	10	155	6
EXP.4	Hooper-2	1.5 × 1.2	Blast Test	15 kg C4	13	91.2	6
EXP.5	Morison-1	1.25 × 1.55	Blast Test	60 kg TNT	12	59	7
EXP.6	Morison-2	1.25 × 1.55	Shock tube	eqiv.100 kg TNT	31	58	14.5
EXP.7	Morison-3	1.25 × 1.55	Shock tube	eqiv.500 kg TNT	65	42	27.8
EXP.8	Kranzer-1	1.1 × 0.9	Blast Test	0.125 kg PETN	2	60	20

3.2. Experimental Program

3.2.1. Arena Blast Testing

In this study, to validate the accuracy of modeling the fracture pattern and the performance condition, the results of an arena blast testing conducted by RedGuard were obtained. This test featured a laminated glass unit attached to an 8 ft × 20 ft (2.44 m × 6.1 m) blast-resistant modular building (BRM). The BRM unit was placed on the natural ground

without restraining/anchoring. The tested laminated glass (LG) unit has the dimensions 36 in × 36 in (915 mm × 915 mm) with an approximate nominal thickness of 2 in (51.5 mm). The glazing unit was attached to the front face of the blast-resistant modular building at the center (Figure 3). The configuration of the tested laminated glass is given in Table 5. This configuration was designed using WINGUARD software. Moreover, to validate the accuracy of the modeling in predicting the performance of the glazing unit under various exposures, the configuration was designed to receive two successive blast tests, passing the first test with minimal damage of 1-2 performance criteria while failing at the second test with a performance criterion of 5 as per GSA-TS01-2003.

Figure 3. Front view (Explosion side) of the BRM unit and the tested LG unit

For this test, the BRM unit's interior was equipped with multiple pressure gauges, witness plates, an accelerometer, and a high-speed camera (Figure 4). Multiple Free-Field Pencil Probes with Decibel Meters were installed on the testing site to record the blast wave. The BRM unit's responses were recorded via a Linear encoder (Figure 5). Furthermore, multiple pressure sensors were installed to record the reflected pressure (front, top, rear, and side of the BRM unit). Finally, the front face of the BRM unit was painted with Chartek-2218 epoxy passive fire protective (PFP) coating.

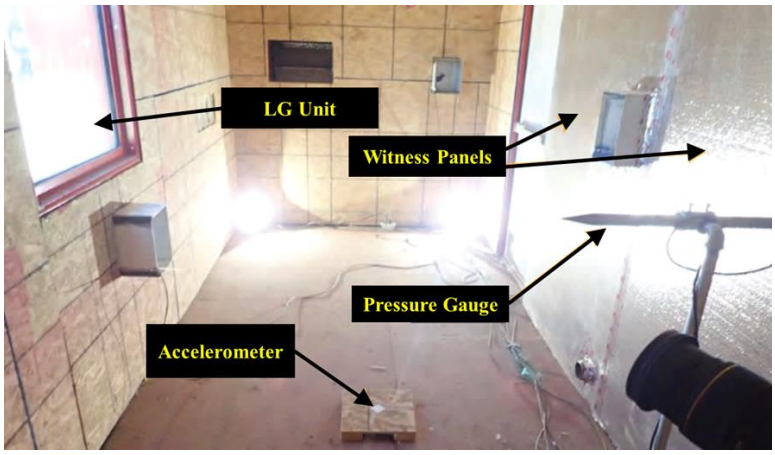

Figure 4. The setup inside the blast-resistant modular unit before testing

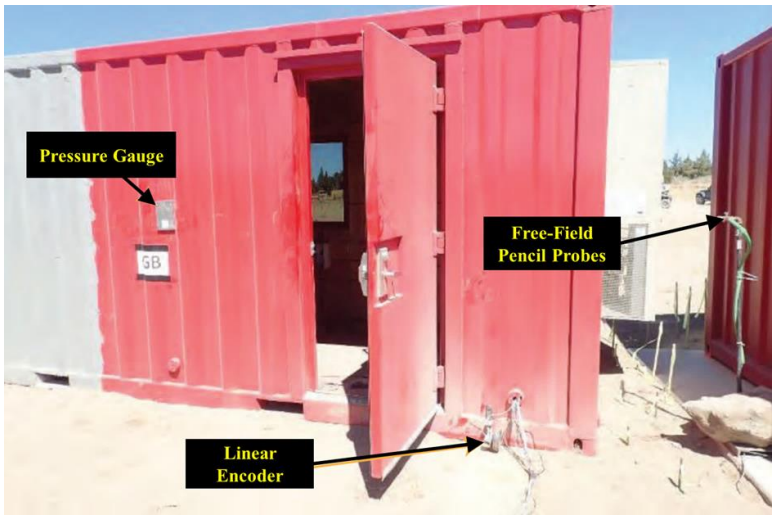

Figure 5. Rear view of the Blast resistant modular unit before testing and allocation of sensors

3.2.2. The Testing Program

This section presents the testing results of two successive blast tests conducted following the Standard Test Method for Glazing Systems by the General Service Administration (GSA). These results are implemented in validating the modeling techniques in the following sections. The GSA standard utilizes the ISC Security Design Criteria to evaluate the effectiveness of window systems when subjected to blast loads. The degree of protection and related hazard levels are classified according to performance conditions summarized in Table 8. These conditions are established based on the post-testing position of the glass fragments and debris in relation to the initial location of the window prior to the blast test.

Table 8. GSA / ISC performance conditions for window system response (GSA-TS01-2003)

Performance Condition	Protection Level	Hazard Level	Description of Window Glazing Response
1	Safe	None	Glazing does not break. No visible damage to glazing or frame.
2	Very high	None	Glazing cracks but is retained by the frame. Dusting or very small fragments near sill or on floor acceptable.
3a	High	Very low	Glazing cracks. Fragments enter space and land on floor no further than 3.3 ft (1 m) from the window.
3b	High	Low	Glazing cracks. Fragments enter space and land on floor no further than 10 ft (3 m) from the window.
4	Medium	Medium	Glazing cracks. Fragments enter space and land on floor and impact a vertical witness panel at a distance of no more than 10 ft (3 m) from the window at a height no greater than 2 ft (0.61 m) above the floor.
5	Low	High	Glazing cracks and window system fails catastrophically. Fragments enter space impacting a vertical witness panel at a distance of no more than 10 ft (3 m) from the window at a height greater than 2 ft (0.61 m) above the floor.

In this study, the LG unit was tested against two successive explosions positioned with the layout given in Figure 6. The blast scenarios were designed so that the first test would inflict minimal damage of 1 to 2 performance criteria. Meanwhile, the second test would cause a failure of the LG unit with a performance criterion of 5 as per GSA-TS01-2003 (Figure 6).

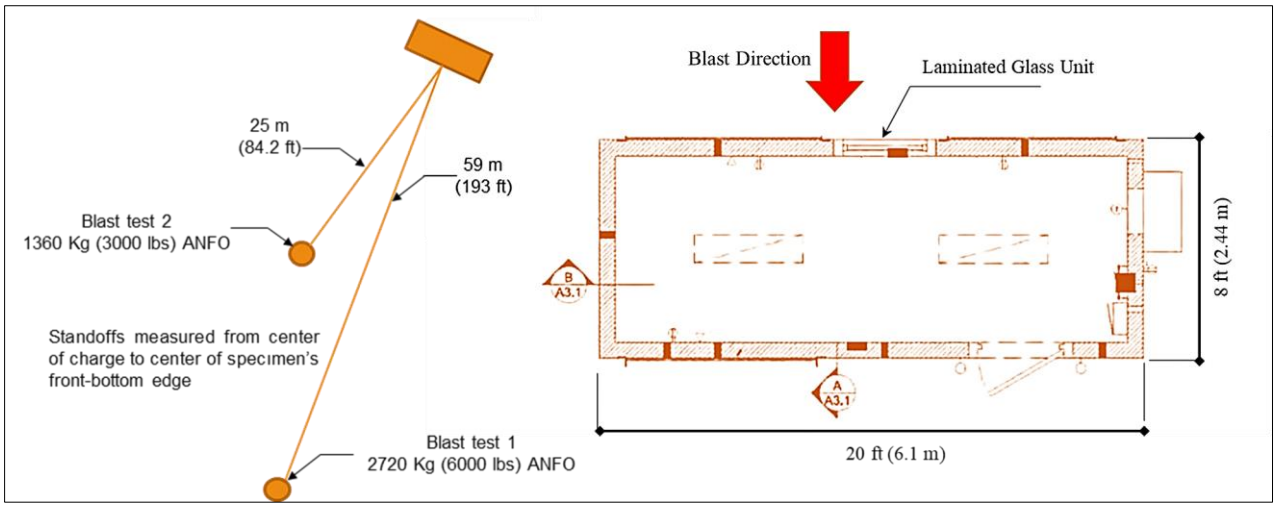

Figure 6. The blast testing site plan and the installation of the laminated glass unit

The first test was conducted with an explosive charge of 6,000 pounds (2720 kg) of ammonium nitrate/fuel oil (ANFO) and with a standoff distance of 193 feet (59 m) to the center of the glazing unit. The second blast test involved an explosive charge of 3,000 pounds (1360 kg) of ANFO (Figure 7). The time-lapse camera feed during the two successive blast tests is shown in Figure 8. The duration of the recorded blast exposures was estimated for the first blast test as 19.7 milliseconds, while the second blast test had a duration of 6.5 milliseconds. The blast tests generated 19.3 psi and 136 psi blast pressures, respectively. The blast wave propagation towards the laminated glass specimen was particularly observed during the second blast test, as depicted in Figure 8.

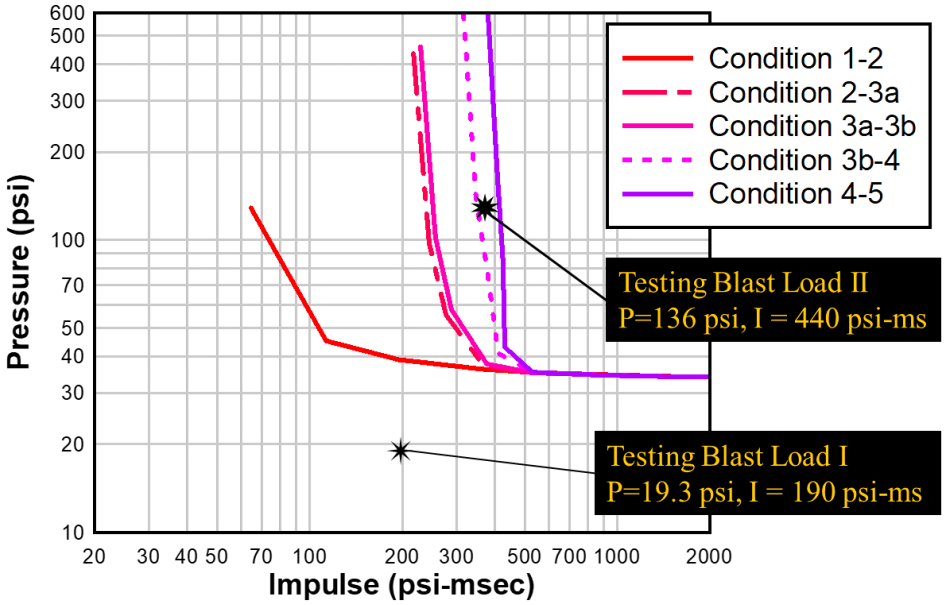

Figure 7. The laminated glass unit design performance criteria during the blast testing

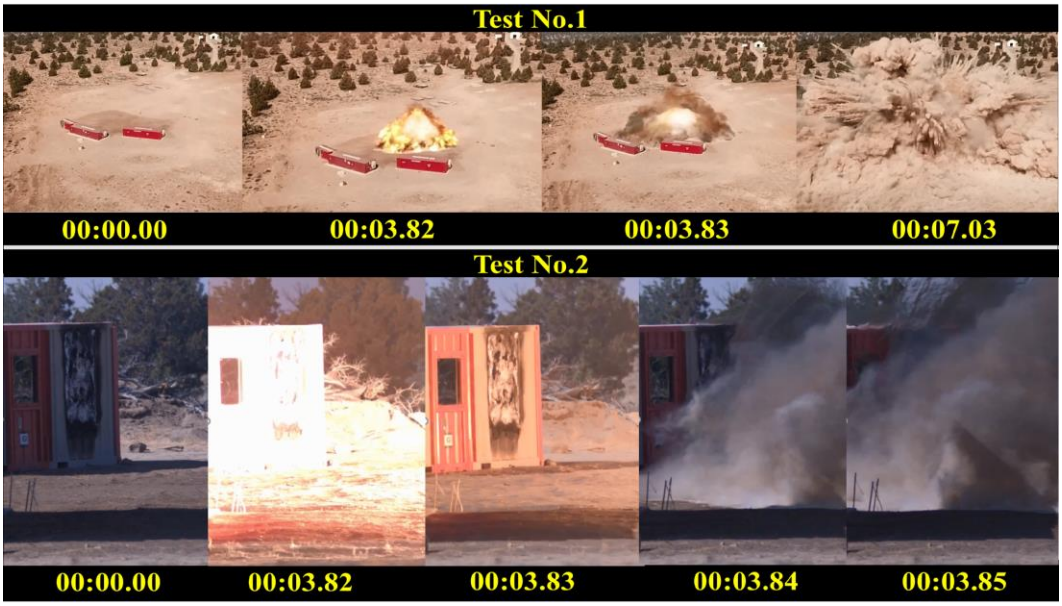

Figure 8. The blast testing sessions and the incident of the blast wave

3.2.3.Post-testing Inspection

Upon inspection, there was no notable structural damage to the BRM unit following the first blast test. This satisfied the requirements for a "Low damage level" rating per the ASCE designations. The laminated glass unit experienced minimal signs of damage, which falls into the first performance criteria as per the GSA- TS01-2003. Meanwhile, the second test failed the laminated glass unit with fragments hitting the witness plate. The results of the two consecutive blast tests are summarized in Table 9. A sample of the recorded pressure time history record from the installed probes is shown in Figure 8 for the second test.

Table 9. The response of the laminated glass following field blast testing

Test ID	Blast Parameters		Performance Condition of LG	Witness Plate Condition	Description of Window Glazing Response
	Pressure (psi)	Duration (m sec)			
Test No.1	19.3	19.7	1	No fragments	No visible damage to the glazing or frame. Glazing did not break.
Test No.2	136	6.5	5	Fragments reached the witness plate	Glazing cracks and window system fails catastrophically. Fragments enter space impacting a vertical witness panel

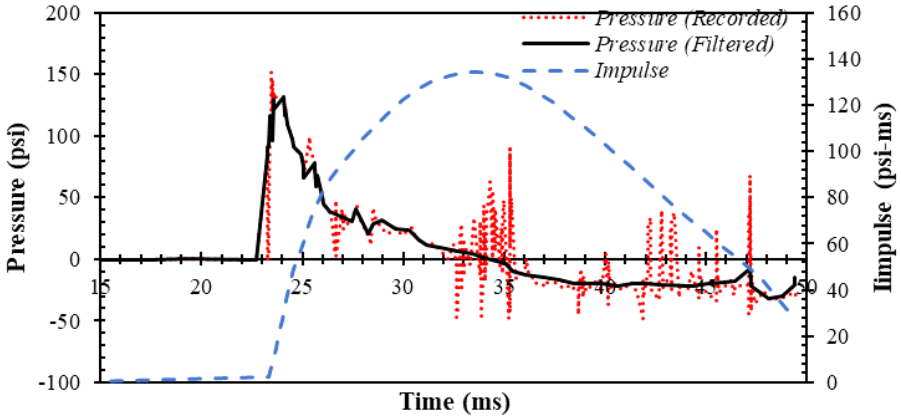

Figure 9. The record of the impulse time history during the blast test

4. Results and Discussion

The laminated glass units are modeled using mesh-based, mesh-free, and hybrid techniques. In this section, a comparison of accuracy and computational cost of the Finite Element Method (FEM); FEM with Element Deletion (FEM-ED); smooth particle hydrodynamics (SPH); and the hybrid Finite Element-smooth particle hydrodynamics (FEM-SPH) is presented.

4.1. Modeling Accuracy

4.1.1. Displacement Modeling

The displacements analyzed in this study pertain specifically to the midpoint of the laminated panel. An extensive modeling endeavour was undertaken to accurately capture the experiments presented in Table 7, comprising numerous executions and meticulous calibration. The modeling efforts were bifurcated into two distinct phases: (1) modeling the behavior up to the ultimate response and (2) modeling the response with the rebound phase. The assessment of the modeling accuracy up to the ultimate response was examined in the case of EXP.1, EXP.3, EXP.6, and EXP.7, as presented in Figure 10. The modeling of these experiments indicates that the employed modeling techniques generally yielded satisfactory results in replicating the peak displacement response. However, several notable considerations emerged during the modeling exercise.

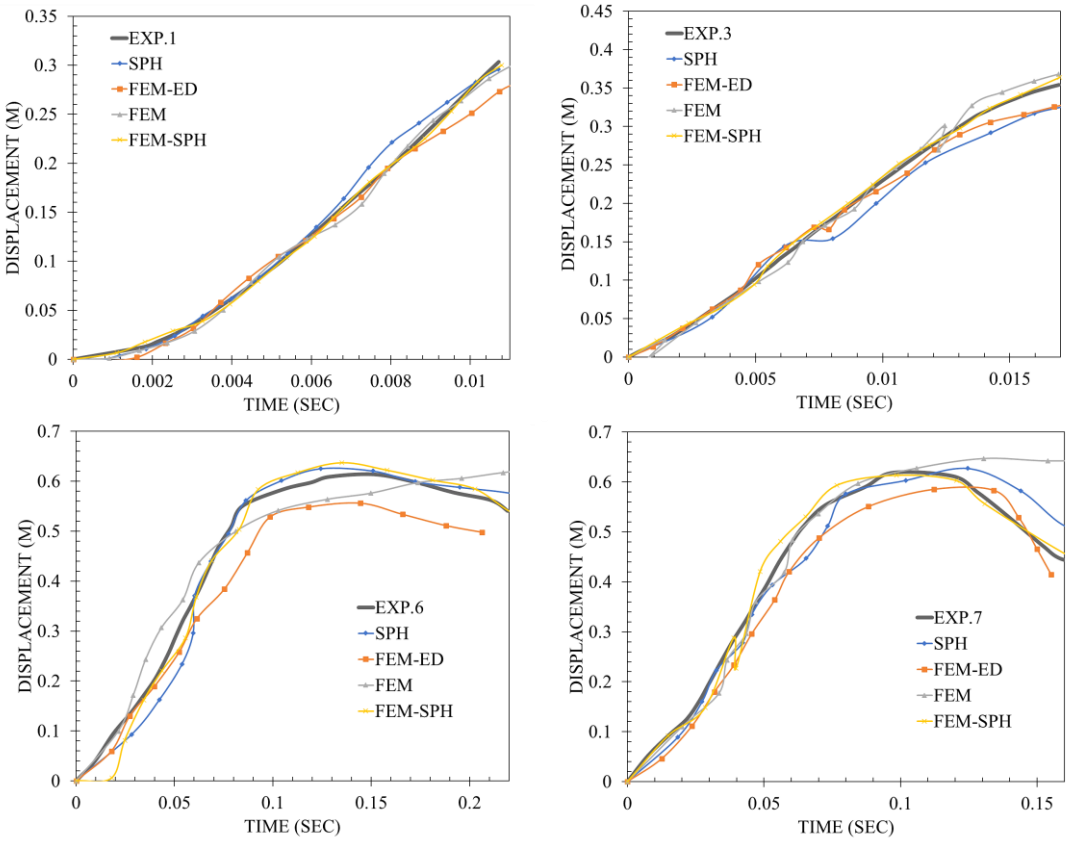

Figure 10. Modeling the laminated glass response up to the ultimate response

Initially, it was observed that the absence of a well-defined re-meshing rule in the Finite Element Method (FEM) modeling led to minor instances of divergence at the peak response, attributable to the onset of excessive mesh distortion. Moreover, among the array of modeling techniques employed, both the hybrid approaches integrating FEM with Element Deletion (FEM-ED) and Smoothed Particle Hydrodynamics (FEM-SPH) demonstrated superior accuracy in capturing the response characteristics of the laminated glass panel. Specifically, the FEM-ED technique exhibited a lower-bound response curve, which marginally underestimated the overall response owing to the removal of elements and subsequent dissipation of energy absorbed by the deleted elements. Conversely, the FEM-SPH approach demonstrated a slight amplification of the response due to the localized energy concentration within the particles. This discrepancy can be mitigated by meticulously formulating the interaction between the free particles and the continuum medium. Notably, the full SPH modeling technique exhibited a more pronounced issue regarding localized energy absorption and an associated overestimation of the response. Nonetheless, employing the aforementioned modeling strategies allows for a satisfactory agreement with the experimental findings.

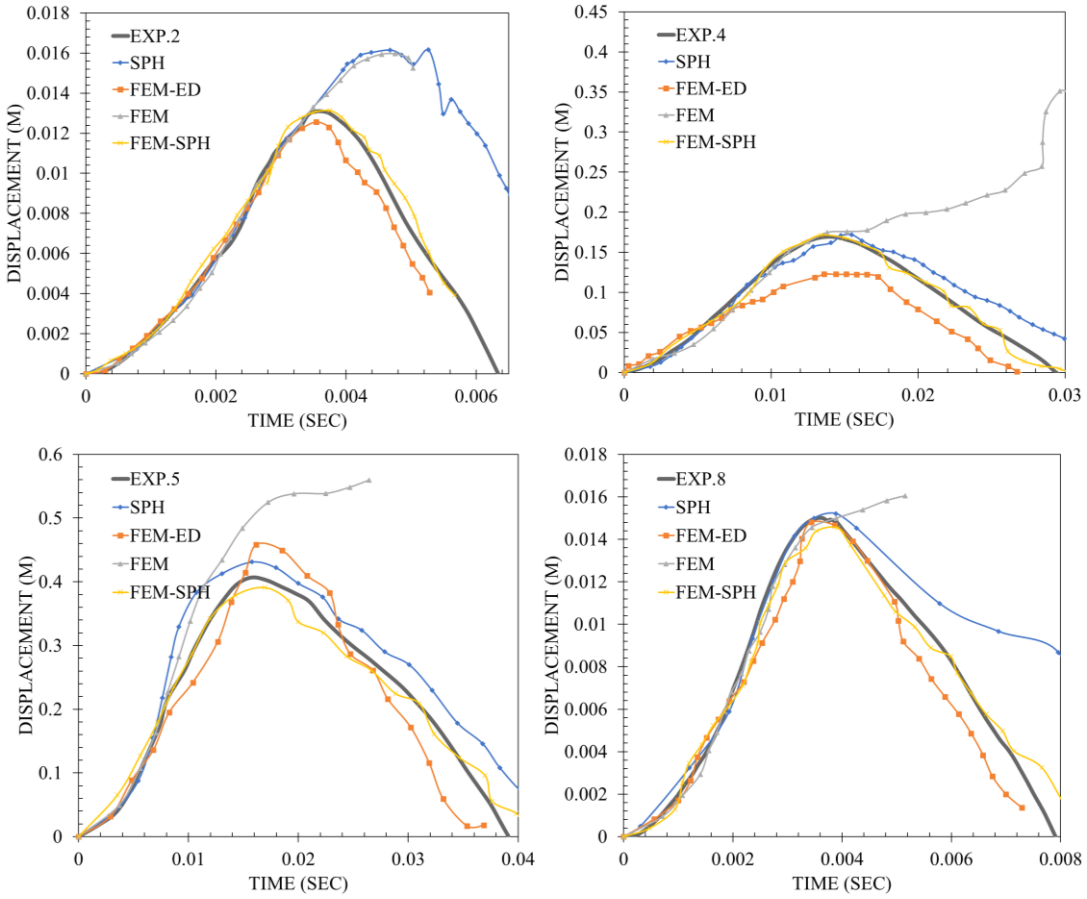

Figure 11. Modeling the rebounding response of laminated glass

In contrast, the hybrid methods (FEM-ED and FEM-SPH) exhibited superior accuracy in capturing the rebound response. However, implementing the FEM-ED exhibits a minor inclination to underestimate the observed response. This underestimation was particularly evident in the case of EXP.4, where the interlayer experienced significant tensile strains. In such instances, the experimental response surpassed the predictions generated using the FEM-ED technique, emphasizing the limitations of this approach.

4.1.2. Fracture Pattern and Fragmentation Modeling

This section focuses on the modeling of fracture patterns and fragmentation in laminated glass using two hybrid techniques: the Finite Element Method with Element Deletion (FEM-ED) and the Finite Element Method with Smoothed Particle Hydrodynamics (FEM-SPH). The results of the numerical simulations are evaluated against experimental data (EXP.8) and the experimental testing program conducted in this study (Test.1 and Test.2), respectively.

4.1.2.1. Effect of Mesh Size

To investigate the effect of mesh size on the modeled response, a record of the back side of EXP.8 is depicted in Figure 12-c. This record was modeled with a coarse mesh (element size 30 mm) as shown in Figure 12-a. A very fine mesh modeling (element size less than 0.1 mm) of this experiment was performed by Larcher et al. [62], as shown in Figure 12(b). The results suggest that a coarse mesh can still predict the prominent diagonal cracks at a mesh size of 1/30 of the panel size. However, it is observed that the accuracy of the FEM-ED technique is highly influenced by the

characteristics of the mesh employed, particularly the type and size of the finite elements. Implementing FEM-ED requires delicate meshing, as the predicted cracking pattern depends on the mesh quality. A relatively fine meshing is required to capture fine cracking (less than or equal to 1/5000 of the panel size). This is attributed to the proportional relationship between the dissipated energy resulting from element deletion and the size of the finite elements.

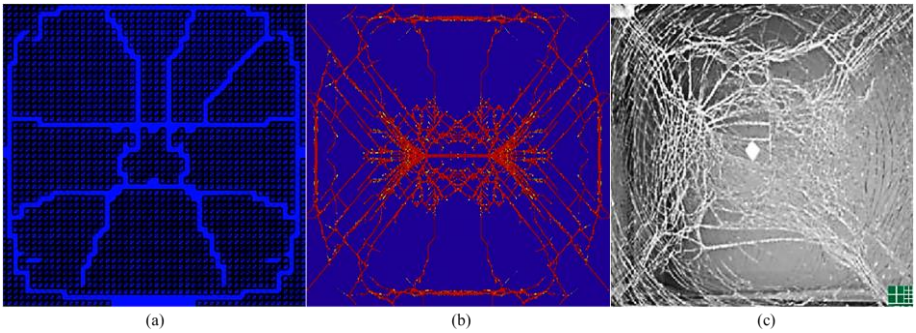

Figure 12. Modeling cracking pattern of EXP.8 with FEM-ED, (a) coarse mesh, (b) fine mesh [62], and (c) experimental results by Kranzer et al. [7]

4.1.2.2. Fragmentation Prediction

By utilizing the hybrid implementation of the FEM-SPH technique, a comprehensive evaluation of laminated glass performance, fracture pattern, fragmentation, and performance condition can be achieved. However, due to its reliance on element deletion, the FEM-ED technique does not account for fragmentation phenomena.

In this study, the FEM-SPH technique has been investigated by modeling cracking patterns and performance conditions recorded on the back side of TEST.1 and TEST.2. The findings are presented in Table 10 and Figure 13 for the performance conditions and the cracking pattern, respectively. It can be seen that the FEM-SPH is capable of predicting fragmentation hazards and the performance conditions of a given laminated glass. Furthermore, FEM-SPH could capture the prominent cracks along the diagonal line of the laminated glass and minor cracks at a medium particle density corresponding to an initial mesh size of 1/20 of the panel's short dimension (25 mm).

Table 10. Predicting the performance conditions of laminated glass using FEM-SPH per GSA-TS01-2003

Instance	Performance Condition	Protection Level	Hazard Level
Test No.1 Experimental	1	Safe- Very high	None
Test No.2 Experimental	5	Low	High
Test No.1 Modeling	1 (three runs)	Safe- Very high	None
Test No.2 Modeling	4-5 (three runs)	Low	High

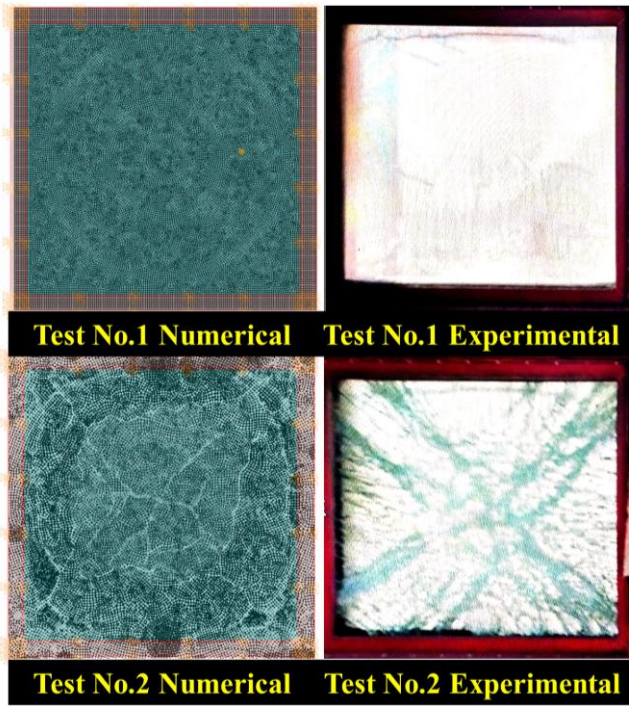

Figure 13. Modeling cracking pattern with FEM-SPH

The capacity of the FEM-SPH technique to generate a higher number of cracks that are more uniformly distributed throughout the laminated glass specimens is attributed to the system's energy retained in the particles, thus circumventing the sudden energy loss encountered in the FEM-ED technique. These particles remain attached to the interlayer until the strain energy surpasses the cohesive contact limit, at which point detachment from the glass panel occurs. The results, presented in Figures 12 and 13, and Table 10, highlight the ability of both modeling techniques to accurately predict the initiation and propagation of cracks, mesh size sensitivity, and fragmentation within the laminated glass specimens.

4.2. Computational Efficiency

Modeling the response of laminated glass to extreme loading scenarios is a computationally intensive task in designing and analyzing protective structures. Therefore, an optimal modeling approach must carefully balance accuracy with computational resources. This study employed a typical four physical Intel(R) Core (TM) i7-8550U CPU @ 1.80 GHz processor with 12 GB RAM. Moreover, GPU processing capabilities were not employed in this investigation. The optimization was done by incrementally tuning the number of processing cores and the threads implemented. The CPU and memory usage percentages, as well as the CPU time during each simulation trial, were recorded. The mean and maximum encountered figures are presented in Table 11. Furthermore, to directly correlate the computational demand with accuracy, the measured mean and maximum percent error based on the displacement estimate at the mid-span of the laminated glass unit was amended to Table 11. The expression used to estimate the percent error is presented in Equation 1, where y_0 is the experimental displacement while y_1 is the numerical approximation of the displacement response.

$$Percent\ Error = \left|\frac{(y_0 - y_1)}{y_0}\right| \times 100 \quad (1)$$

Table 11. The computational performance of the modeling techniques

Measurement		Process CPU Usage	Process Memory Used	CPU time (sec)	Percent Error
FEM	Average	69%	75%	840	13%
	Maximum	91%	94%	2880	29%
SPH	Average	65%	73%	960	11%
	Maximum	93%	93%	3540	30%
FEM-ED	Average	60%	70%	750	6%
	Maximum	84%	97%	1860	14%
FEM-SPH	Average	72%	79%	870	5%
	Maximum	90%	97%	2100	12%

It was observed that the capability of multiprocessing allows for efficient deployment of the hybrid techniques to approach the time required with the FEM technique. The efficient deployment of the FEM-ED and FEM-SPH can provide the best accuracy for maximum displacement with a percent error as low as 6% and 5%, respectively.

5. Conclusion

This study evaluates various modeling techniques for analyzing laminated glass responses to blast loading, highlighting their effectiveness and limitations. The investigation encompasses two modeling phases: pre-ultimate response and rebound behaviour.

In the pre-ultimate response phase Finite Element Method (FEM) modeling demonstrated limitations due to mesh distortion without re-meshing rules. In contrast, hybrid methods like FEM with Element Deletion (FEM-ED) and Smoothed Particle Hydrodynamics (FEM-SPH) exhibited superior accuracy. FEM-ED provided lower-bound responses, influenced by element removal and energy dissipation, and whereas FEM-SPH showed slight amplification due to localized energy concentration. Adaptive meshing improved FEM-ED accuracy. Meanwhile, full SPH modeling exhibited localized energy absorption but generally aligned with experimental data.

In the rebound phase, FEM faced challenges due to mesh distortion, while SPH occasionally overestimated damage. Hybrid approaches, especially FEM-ED and FEM-SPH, achieved higher accuracy. All modeling techniques effectively predicted cracking initiation and propagation. FEM-ED's accuracy depended on mesh quality, while FEM-SPH resulted in a higher number of uniformly distributed cracks. The hybrid FEM-SPH approach allowed comprehensive evaluation but did not account for fragmentation. Resource analysis, including CPU and memory usage percentages and CPU time (Table 11), provided valuable insights into resource-accuracy trade-offs, contributing to the understanding of laminated glass modeling for protective structure design.

In summary, this research informs the choice of modeling techniques for studying laminated glass responses to extreme loading scenarios. It highlights the strengths and limitations of each approach, aiding in the design and analysis of protective laminated glass.

5.1. Limitations and Future Research

This study primarily focuses on the response of laminated glass to high-strain rates and short-duration blast scenarios. Future research could enhance the applicability of the modeling techniques to static and quasi-static loading conditions by incorporating more computationally demanding material models, especially for the interlayers exhibiting hyperelastic and viscoelastic responses. Anticipated impacts include alterations in both accuracy and computational cost. Additionally, the dataset utilized in this study is limited in its range of explosion loads and features consistent structural dimensions. Future research opportunities lie in exploring the effects of varying load characteristics and geometries on accuracy and computational demand. Addressing these limitations will examine the applicability of the presented conclusions, ultimately advancing the field of blast-resistant materials and structural design.

6. Declarations

6.1. Author Contributions

Conceptualization, M.H. and A.S.; methodology, M.H.; software, M.H.; validation, M.H. and A.S.; formal analysis, M.H.; investigation, M.H.; resources, M.H.; data curation, M.H.; writing—original draft preparation, M.H.; writing—review and editing, M.H.; visualization, M.H.; supervision, A.S.; project administration, M.H.; funding acquisition, M.H. All authors have read and agreed to the published version of the manuscript.

6.2. Data Availability Statement

The data presented in this study are available on request from the corresponding author.

6.3. Funding

This work was conducted with the financial assistance of the Istanbul Technical University Research Fund under the scope of BAP Project Number 43460, which is gratefully acknowledged.

6.4. Acknowledgements

The authors would like to express their gratitude for the support received during this research project. This work was conducted with the financial assistance of the Istanbul Technical University Research Fund under the scope of BAP Project Number 43460, which is gratefully acknowledged. Furthermore, the authors acknowledge the valuable contribution of RedGuard for providing the arena testing results used in this research. The authors also acknowledge the support of Şişecam for conducting the glass material testing for mechanical properties.

6.5. Conflicts of Interest

The authors declare no conflict of interest.

7. References

[1] Chen, S., Zang, M., Wang, D., Yoshimura, S., & Yamada, T. (2017). Numerical analysis of impact failure of automotive laminated glass: A review. Composites Part B: Engineering, 122, 47–60. doi:10.1016/j.compositesb.2017.04.007.

[2] Teotia, M., & Soni, R. K. (2018). Applications of finite element modelling in failure analysis of laminated glass composites: A review. Engineering Failure Analysis, 94, 412–437. doi:10.1016/j.engfailanal.2018.08.016.

[3] US7611773B2. (2009). Glass Composition and Laminated Glass. US Patent, Alexandria, United States.

[4] Castori, G., & Speranzini, E. (2017). Structural analysis of failure behavior of laminated glass. Composites Part B: Engineering, 125, 89–99. doi:10.1016/j.compositesb.2017.05.062.

[5] Wu, G., & Yang, J. M. (2005). The mechanical behavior of GLARE laminates for aircraft structures. Failure in Structural Materials, 57(1), 72–79. doi:10.1007/s11837-005-0067-4.

[6] Vedrtnam, A. (2019). Novel treatment methods for improving fatigue behavior of laminated glass. Composites Part B: Engineering, 167, 180–198. doi:10.1016/j.compositesb.2018.12.037.

[7] Kranzer, C., Gürke, G., & Mayrhofer, C. (2005). Testing of bomb resistant glazing systems. Experimental investigation of the time dependent deflection of blast loaded 7.5 mm laminated glass. Glass processing days (June 2005). Tampere, Finland.

[8] Biolzi, L., Cattaneo, S., Orlando, M., Piscitelli, L. R., & Spinelli, P. (2018). Post-failure behavior of laminated glass beams using different interlayers. Composite Structures, 202, 578–589. doi:10.1016/j.compstruct.2018.03.009.

[9] Lu, Y., Zhao, S., & Chen, S. (2023). Compressive buckling performance of multilayer laminated glass columns with different interlayers. Engineering Structures, 281. doi:10.1016/j.engstruct.2023.115701.

[10] Schuster, M. (2022). Characterization of laminated safety glass interlayers: thermorheology, crystallinity and viscoelasticity. Technische Universität Darmstadt, 341. doi:10.26083/tuprints-00021741.

[11] Rühl, A., Kolling, S., & Schneider, J. (2017). Characterization and modeling of poly(methyl methacrylate) and thermoplastic polyurethane for the application in laminated setups. Mechanics of Materials, 113, 102–111. doi:10.1016/j.mechmat.2017.07.018.

[12] Kraus, M. A. (2019). Machine learning techniques for the material parameter identification of laminated glass in the intact and post-fracture state. Thesis, University of the Bundeswehr Munich, Neubiberg, Germany.

[13] Chen, X., Rosendahl, P. L., Chen, S., & Schneider, J. (2021). On the delamination of polyvinyl butyral laminated glass: Identification of fracture properties from numerical modelling. Construction and Building Materials, 306(124827). doi:10.1016/j.conbuildmat.2021.124827.

[14] Del Linz, P., Hooper, P. A., Arora, H., Wang, Y., Smith, D., Blackman, B. R. K., & Dear, J. P. (2017). Delamination properties of laminated glass windows subject to blast loading. International Journal of Impact Engineering, 105, 39–53. doi:10.1016/j.ijimpeng.2016.05.015.

[15] Foraboschi, P. (2012). Analytical model for laminated-glass plate. Composites Part B: Engineering, 43(5), 2094–2106. doi:10.1016/j.compositesb.2012.03.010.

[16] Baraldi, D., Cecchi, A., & Foraboschi, P. (2016). Broken tempered laminated glass: Non-linear discrete element modeling. Composite Structures, 140, 278–295. doi:10.1016/j.compstruct.2015.12.050.

[17] Shahriari, M., & Saeidi Googarchin, H. (2020). Prediction of vehicle impact speed based on the post-cracking behavior of automotive PVB laminated glass: Analytical modeling and numerical cohesive zone modeling. Engineering Fracture Mechanics, 240. doi:10.1016/j.engfracmech.2020.107352.

[18] Seyedalikhani, S., Shokrieh, M. M., & Shamaei-Kashani, A. R. (2020). A novel dynamic constitutive micromechanical model to predict the strain rate dependent mechanical behavior of glass/epoxy laminated composites. Polymer Testing, 82. doi:10.1016/j.polymertesting.2019.106292.

[19] Biolzi, L., Casolo, S., Orlando, M., & Tateo, V. (2019). Modelling the response of a laminated tempered glass for different configurations of damage by a rigid body spring model. Engineering Fracture Mechanics, 218. doi:10.1016/j.engfracmech.2019.106596.

[20] Malewski, A., Kozłowski, M., Podwórny, J., Środa, M., & Sumelka, W. (2023). Developments on Constitutive Material Model for Architectural Soda-Lime Silicate (SLS) Glass and Evaluation of Key Modelling Parameters. Materials, 16(1), 397. doi:10.3390/ma16010397.

[21] Zhang, X., Hao, H., & Ma, G. (2015). Dynamic material model of annealed soda-lime glass. International Journal of Impact Engineering, 77, 108–119. doi:10.1016/j.ijimpeng.2014.11.016.

[22] Balan, B. A., & Achintha, M. (2015). Assessment of Stresses in Float and Tempered Glass Using Eigenstrains. Experimental Mechanics, 55(7), 1301–1315. doi:10.1007/s11340-015-0036-y.

[23] Nielsen, J. H., & Bjarrum, M. (2017). Deformations and strain energy in fragments of tempered glass: experimental and numerical investigation. Glass Structures and Engineering, 2(2), 133–146. doi:10.1007/s40940-017-0043-8.

[24] Bonati, A., Pisano, G., & Royer Carfagni, G. (2020). Probabilistic considerations about the strength of laminated annealed float glass. Glass Structures and Engineering, 5(1), 27–40. doi:10.1007/s40940-019-00111-8.

[25] Osnes, K., Børvik, T., & Hopperstad, O. S. (2018). Testing and modelling of annealed float glass under quasi-static and dynamic loading. Engineering Fracture Mechanics, 201, 107–129. doi:10.1016/j.engfracmech.2018.05.031.

[26] Brokmann, C., Alter, C., & Kolling, S. (2023). A Methodology for Stochastic Simulation of Head Impact on Windshields. Applied Mechanics, 4(1), 179–190. doi:10.3390/applmech4010010.

[27] Serafinavičius, T., Lebet, J. P., Louter, C., Lenkimas, T., & Kuranovas, A. (2013). Long-term laminated glass four point bending test with PVB, EVA and SG interlayers at different temperatures. Procedia Engineering, 57, 996–1004. doi:10.1016/j.proeng.2013.04.126.

[28] Rivers, G., & Cronin, D. (2019). Influence of moisture and thermal cycling on delamination flaws in transparent armor materials: Thermoplastic polyurethane bonded glass-polycarbonate laminates. Materials and Design, 182(108026). doi:10.1016/j.matdes.2019.108026.

[29] Parratt, M. (2016). Behaviour of Multi-Layered Laminated Glass under Blast Loading. Master Thesis, University of Toronto, Toronto, Canada.

[30] Kuntsche, J., & Schneider, J. (2014). Mechanical behaviour of polymer interlayers in explosion resistant glazing. In Challenging Glass 4 and COST Action TU0905 Final Conference - Proceedings of the Challenging Glass 4 and Cost Action TU0905 Final Conference, 447–454. doi:10.1201/b16499-65.

[31] Angelides, S. C. (2022). Blast Resilience of Glazed Façades: Towards a New Understanding of the Post-Fracture Behaviour of Laminated Glass. PhD Thesis, University of Cambridge. doi:10.17863/CAM.87476.

[32] Biolzi, L., Cattaneo, S., Orlando, M., Piscitelli, L. R., & Spinelli, P. (2020). Constitutive relationships of different interlayer materials for laminated glass. Composite Structures, 244(112221). doi:10.1016/j.compstruct.2020.112221.

[33] Zhang, L. H., Yao, X. H., Zang, S. G., & Han, Q. (2015). Temperature and strain rate dependent tensile behavior of a transparent polyurethane interlayer. Materials and Design, 65, 1181–1188. doi:10.1016/j.matdes.2014.08.054.

[34] Biolzi, L., Cattaneo, S., & Rosati, G. (2010). Progressive damage and fracture of laminated glass beams. Construction and Building Materials, 24(4), 577–584. doi:10.1016/j.conbuildmat.2009.09.007.

[35] Gao, W., Xiang, J., Chen, S., Yin, S., Zang, M., & Zheng, X. (2017). Intrinsic cohesive modeling of impact fracture behavior of laminated glass. Materials and Design, 127, 321–335. doi:10.1016/j.matdes.2017.04.059.

[36] Alter, C., Kolling, S., & Schneider, J. (2017). A new failure criterion for laminated safety glass. 11th European LS-Dyna Conference, 9-11 May, 2017, Salzburg, Austria.

[37] El-Sisi, A., Newberry, M., Knight, J., Salim, H., & Nawar, M. (2022). Static and high strain rate behavior of aged virgin PVB. Journal of Polymer Research, 29(2), 39. doi:10.1007/s10965-021-02876-5.

[38] Chen, X., Chen, S., & Li, G. (2021). Failure Mode of Framed Polyvinyl-Butyral-Laminated Glass Subjected to Blast Loading. Tongji Daxue Xuebao/Journal of Tongji University, 49(11), 1565–1574. doi:10.11908/j.issn.0253-374x.20306.

[39] Hidallana-Gamage, H. D., Thambiratnam, D. P., & Perera, N. J. (2014). Numerical modelling and analysis of the blast performance of laminated glass panels and the influence of material parameters. Engineering Failure Analysis, 45, 65–84. doi:10.1016/j.engfailanal.2014.06.013.

[40] Wang, X. E., Yang, J., Liu, Q. F., Zhang, Y. M., & Zhao, C. (2017). A comparative study of numerical modelling techniques for the fracture of brittle materials with specific reference to glass. Engineering Structures, 152, 493–505. doi:10.1016/j.engstruct.2017.08.050.

[41] Literature survey General (1985). A review of the literature on finite-element modelling of laminated composite plates. Composites, 16(4), 337. doi:10.1016/0010-4361(85)90318-0.

[42] Jaśkowiec, J. (2015). Numerical Modeling Mechanical Delamination in Laminated Glass by XFEM. Procedia Engineering, 108, 293–300. doi:10.1016/j.proeng.2015.06.150.

[43] Sun, X., Khaleel, M. A., & Davies, R. W. (2005). Modeling of Stone-impact Resistance of Monolithic Glass Ply Using Continuum Damage Mechanics. International Journal of Damage Mechanics, 14(2), 165–178. doi:10.1177/1056789505048601.

[44] Ismail, J., Zaïri, F., Naït-Abdelaziz, M., Bouzid, S., & Azari, Z. (2011). Experimental and numerical investigations on erosion damage in glass by impact of small-sized particles. Wear, 271(5–6), 817–826. doi:10.1016/j.wear.2011.03.009.

[45] Lenk, P., & Lambert, H. (2015). Practical aspects of finite-element analysis in structural glass design. Proceedings of the Institution of Civil Engineers - Structures and Buildings, 168(7), 527–538. doi:10.1680/stbu.13.00104.

[46] Gao, W., & Zang, M. (2014). The simulation of laminated glass beam impact problem by developing fracture model of spherical DEM. Engineering Analysis with Boundary Elements, 42, 2–7. doi:10.1016/j.enganabound.2013.11.011.

[47] Wang, X., Yang, J., Pan, Z., Wang, F., Meng, Y., & Zhu, Y. (2021). Exploratory investigation into the post-fracture model of laminated tempered glass using combined Voronoi-FDEM approach. International Journal of Mechanical Sciences, 190, 105989. doi:10.1016/j.ijmecsci.2020.105989.

[48] Nikbakt, S., Kamarian, S., & Shakeri, M. (2018). A review on optimization of composite structures Part I: Laminated composites. Composite Structures, 195, 158–185. doi:10.1016/j.compstruct.2018.03.063.

[49] Zhou, Y., Sun, Y., Huang, T., & Cai, W. (2019). SPH-FEM simulation of impacted composite laminates with different layups. Aerospace Science and Technology, 95, 105469. doi:10.1016/j.ast.2019.105469.

[50] Zhou, Y., Sun, Y., & Cai, W. (2019). Bird-striking damage of rotating laminates using SPH-CDM method. Aerospace Science and Technology, 84, 265–272. doi:10.1016/j.ast.2018.10.009.

[51] Grimaldi, A., Sollo, A., Guida, M., & Marulo, F. (2013). Parametric study of a SPH high velocity impact analysis – A birdstrike windshield application. Composite Structures, 96, 616–630. doi:10.1016/j.compstruct.2012.09.037.

[52] Spiller, K., Packer, J. A., Seica, M. V., & Yankelevsky, D. Z. (2016). Prediction of annealed glass window response to blast loading. International Journal of Impact Engineering, 88, 189–200. doi:10.1016/j.ijimpeng.2015.10.010.

[53] Norville, H. S., & Conrath, E. J. (2001). Considerations for Blast-Resistant Glazing Design. Journal of Architectural Engineering, 7(3), 80–86. doi:10.1061/(asce)1076-0431(2001)7:3(80).

[54] Bedon, C., Larcher, M., Bez, A., & Amadio, C. (2022). Numerical Analysis of TGU Windows under Blast - Glass-Shard Outlook. Challenging Glass 8: Conference on Architectural and Structural Applications of Glass, CGC 2022, 8. doi:10.47982/cgc.8.450.

[55] Cao, K., Wang, Y., & Wang, Y. (2012). Effects of strain rate and temperature on the tension behavior of polycarbonate. Materials and Design, 38, 53–58. doi:10.1016/j.matdes.2012.02.007.

[56] Jayaweera, G. C. S., Hidallana-Gamage, H. D., & Baleshan, B. (2022). Case Studies on Blast Behaviour of Glass Façades: Sri Lanka Easter Bombings. IEEE, 2022 Moratuwa Engineering Research Conference (MERCon), Moratuwa, Sri Lanka, 1-6. doi:10.1109/mercon55799.2022.9906182.

[57] Saflex. (2023). Saflex Clear Technical Datasheet. Eastman Chemical Company, Tennessee, United States. Available online: https://www.saflex.com/technical-documents (accessed on May 2023).

[58] Huntsman. (2023). KRYSTALFLEX TPU Films for Safety Glazing Applications. Huntsman International LLC, Utah, United States. Available online: https://www.huntsman.com/products/detail/313/krystalflex (accessed on May 2023).

[59] Zhang, X., & Hao, H. (2015). Experimental and numerical study of boundary and anchorage effect on laminated glass windows under blast loading. Engineering Structures, 90, 96–116. doi:10.1016/j.engstruct.2015.02.022.

[60] Wang, K. G., Lea, P., & Farhat, C. (2015). A computational framework for the simulation of high-speed multi-material fluid-structure interaction problems with dynamic fracture. International Journal for Numerical Methods in Engineering, 104(7), 585–623. doi:10.1002/nme.4873.

[61] Morison, C. (2007). The resistance of laminated glass to blast pressure loading and the coefficients for single degree of freedom analysis of laminated glass. Ph.D. Thesis, Cranfield University, Cranfield, United Kingdom.

[62] Larcher, M., Solomos, G., Casadei, F., & Gebbeken, N. (2012). Experimental and numerical investigations of laminated glass subjected to blast loading. International Journal of Impact Engineering, 39(1), 42–50. doi:10.1016/j.ijimpeng.2011.09.006.

[63] Del Linz, P., Hooper, P. A., Arora, H., Smith, D., Pascoe, L., Cormie, D., Blackman, B. R. K., & Dear, J. P. (2015). Reaction forces of laminated glass windows subject to blast loads. Composite Structures, 131, 193–206. doi:10.1016/j.compstruct.2015.04.050.